

## **CONTROL STRATEGIES FOR AUTOMOTIVE RANKINE SYSTEM EVALUATION USING A COSIMULATION PLATFORM**

Abdelmajid Taklanti\*, Jin-Ming LIU, Regine Haller, Samy Hammi, Bertrand Nicolas, Yulia Glavatskaya and Mohamed Yahia

Valeo Thermal Systems  
8, rue Louis Lormand 78321 le Mesnil saint Denis  
Contact Information (abdelmajid.taklanti@valeo.com)

### **ABSTRACT**

Today, several solutions to recover wasted heat in automotive power train are considered and evaluated in order to reduce vehicle fuel consumption and to meet new emission regulation targets (El Habachi *et al.* (2010), Abbe Horst *et al.* (2014), Domingues *et al.* (2013) and Haller *et al.* (2014)). One of the solutions is to use Organic Rankine Cycle to recover waste heat from engine cooling system and/or engine exhaust gas and transform it to mechanical or electrical power. Automotive environment is very severe and very transient, the key point for operating such system is to set up and validate a suitable control strategy to maximize the recovered output power.

In automotive industry development processes the control strategies are mainly described in a control tool environment. Commonly, the control is then tested and the control parameters are set up using physical mockups and prototypes of the studied system on a test bench. Afterwards the control is coded into a control unit and integrated in a vehicle or a demo-car in order to validate and tune up the control strategies and parameters. This process is very long and time consuming because physical prototype and demo-car are needed.

In this paper, we are going to present a methodology using a virtual model of a R134a low temperature Rankine system integrated in a vehicle platform developed in a system simulation tool environment and coupled to a Rankine control system developed in a control tool environment. This methodology and co-simulation (see Taklanti *et al.*, 2013) allow us to test and evaluate different control strategies, to select the optimal one and to set up control parameters prior to physical mockup or demo car availability.

Finally, some results are presented showing the performance of a low temperature R134a Rankine system in a vehicle environment and the performance of a control strategy for constant velocities and transient driving cycles.

### **1 INTRODUCTION**

The efficiency of an Internal Combustion Engine used in passenger cars is at maximum 45% and about 18% in average during the NEDC driving cycle. This means, 55% to 78% of the chemical energy in the fuel is emitted to the environment as heat through the exhaust line and the engine cooling system. Many investigations have been done to exploit these losses. Direct use of heat to enhance engine warm up, thermoelectricity, turbo-compound, for example, are technical solutions mainly valorizing the exhaust losses. Among those technologies, Rankine Cycle seems very promising and potentially able to use low or high temperature heat losses considering a well adapted working fluid and component technologies.

Haller *et al.* (2014) compared Rankine waste heat recovery system performance versus car velocity at high and low heat source temperature. It appears that the low temperature system is better than the high temperature one at lower engine loads which corresponds to lower vehicle speeds. An additional parameter is the ambient temperature as it affects the performance of the heat sink. The high

temperature system is well adapted for high engine load at high speed driving and less sensitive to ambient condition. Depending on the ambient temperature the crossing point is variable, but approximately at a vehicle speed of 100km/h for an ambient temperature of 22°C.

In this paper the methodology for the control strategy development of the Rankine system and the optimization of the recovered power will be presented. This methodology is applied to a R134a low temperature Rankine system integrated into a vehicle power train.

## 2 R134A LOW TEMPERATURE RANKINE SYSTEM

Different Rankine system architectures are possible for automotive applications. Figure 1 presents the low temperature Rankine system layout chosen for the current study. The engine coolant picks up the waste heat of the engine which is then used to evaporate the working fluid in the water evaporator (or boiler). The expansion of high pressure vapor through the refrigerant expander (RExp) produces mechanical power. Then, the low pressure vapor condenses in the water condenser cooled by a low temperature coolant circuit. Finally a subcooler guarantees sub-cooled liquid at pump inlet to prevent the pump from cavitations.

Exhaust gas heat recovery exchanger (EHR) may be considered in the high temperature coolant loop prior to the evaporator. With higher coolant temperature the potential of recovery power increases and the system efficiency may be improved.

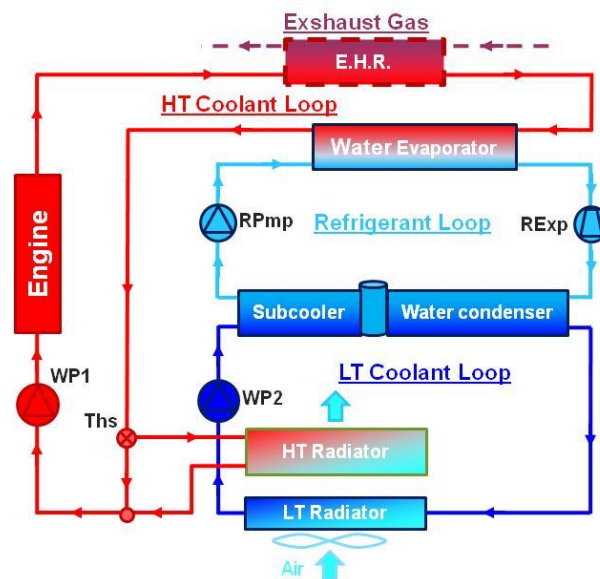


**Figure 1 :** Low temperature Rankine Architecture

For the integration of the Rankine system in a vehicle different solutions are possible. In the architecture considered in this study, the evaporator is placed at engine coolant outlet. The thermostat (Ths) controls the temperature setting at engine outlet by adjusting the coolant flow distribution between high temperature radiator and the radiator bypass. In the low temperature circuit, the electrical water pump WP2 ensures the coolant circulation in the water condenser and subcooler. The low temperature radiator is placed in the vehicle front end upstream, or in parallel of, the high temperature radiator.

## 3 SIMULATION MODEL DEVELOPMENT

### 3.1 R134a Rankine Cycle Model

A simulation model of a R134a Rankine cycle was developed in a multi-physics systems simulation tool. Figure 2 presents a sketch of the Rankine cycle composed of 3 main circuits: High temperature

coolant loop, refrigerant loop and low temperature coolant loop. Those loops integrate the main components of the system: evaporator, expander, condenser, receiver, subcooler, refrigerant pump, low temperature radiator and water pump.

A co-simulation block developed on control tool representing the Rankine control system is linked to the Rankine system model developed on system simulation tool.

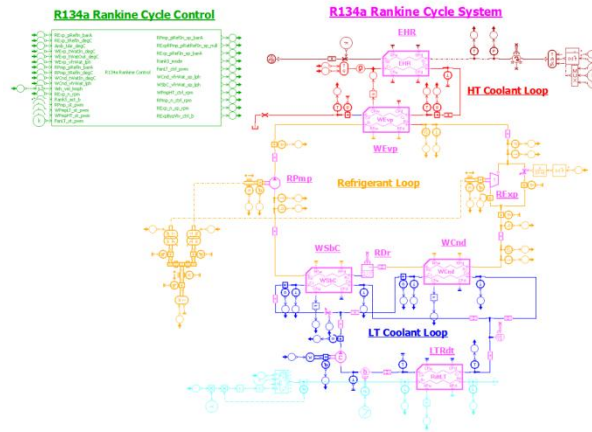


**Figure 2 :** R134a Rankine cycle simulation model

Large experimental investigations were performed on a low temperature Rankine cycle prototype as shown in figure 3 (see also Haller *et al* (2014)). The characteristics of this low temperature R134a Rankine prototype and part of the experimental results were used to set up the simulation model and to define and calibrate parameters of the physical component models.

## 4 R134A RANKINE SYSTEM CONTROL DEVELOPMENT

### 4.1 Rankine System Operation

Figure 3 represents a Rankine cycle operation in R134a Mollier Diagram (temperature/entropy and pressure/enthalpy). The mechanical power recovered by the Expander is:

$$P_{W_{rExp}} = (H_{rExp_i} - H_{rExp_o}) * Q_{m_{rExp}} \quad (1)$$

$$P_{W_{mExp}} = P_{W_{rExp}} * Eff_{mExp} \quad (2)$$

To maximize the recovered power by the expander it is necessary to maximize the product of refrigerant mass flow rate  $Q_{m_{rExp}}$  and the difference between inlet and outlet enthalpy of Expander ( $H_{rExp_i} - H_{rExp_o}$ ) weighted by the Expander mechanical efficiency  $Eff_{mExp}$ . These variables depend on a set of external and internal parameters of the Rankine cycle.

The principal external parameters are:

- Temperature and volume flow rate of the high temperature coolant at evaporator inlet
- Temperature and mass flow rate of ambient air at low temperature radiator

The principal internal parameters are:

- Refrigerant pump speed
- Refrigerant expander speed

Other internal parameters which affect the Rankine system performance are the sizing of the heat exchangers and other components, the volume of the refrigerant loop and the refrigerant charge, volume and mass flow rate of high temperature and low temperature coolant loops.

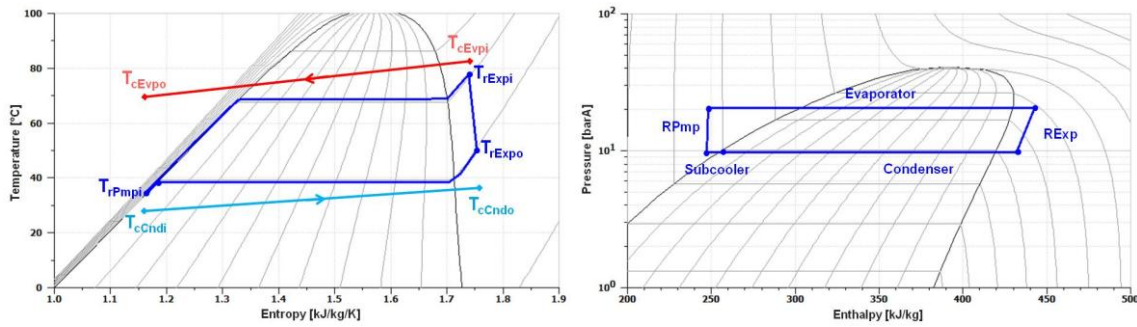


**Figure 3 :** R134a TS and Mollier diagram of Rankine cycle

In practice, maximizing the power  $P_{w_{mExp}}$  of the expander isn't enough, because the refrigerant pump has to be driven electrically or mechanically, in fact we should maximize the net power produced by the Rankine system. This is to say, for a predefined external condition, it is important to control pump and expander speeds in order to maximize the recovered net power  $P_{w_{mNet}}$  defined by:

$$P_{w_{mNet}} = P_{w_{mExp}} - P_{w_{mPmp}} \quad (3)$$

In mean time the control system should ensure the Rankine system protection for all operating points:

1. Avoid that high pressure exceeds a maximal limit  $HP_{work\_max}$ .
2. Ensure a superheat at expander inlet higher than  $Sh_{work\_min}$  and avoid droplets formation at evaporator outlet, since it can damage the expander.
3. Avoid cooling down the coolant at the evaporator outlet below a minimum temperature limit  $T_{w\_out\_min}$ .
4. Ensure a minimum subcooling at pump inlet higher than  $Sb_{work\_min}$  to avoid pump cavitations.

#### 4.2 Optimal Rankine System operation

In order to find the best compromise of pump and expander speeds a matrix of steady state operating conditions is defined. It corresponds to ambient temperatures variation between  $-20^{\circ}C$  and  $+45^{\circ}C$  and vehicle speed variation from 30 to 180 km/h (low temperature radiator air velocity variation from 0.75 m/s to 7 m/s without Fan functioning).

For each external operating condition steady states simulations are performed for a set of pump speeds variation and expander speeds variation. Points with high pressure values exceeding the maximum working pressure  $HP_{work\_max}=32$  bar are removed. The same for points with a superheat at evaporator outlet or condenser inlet lower than  $Sh_{work\_min} = 5$  K. The target of these simulations is to identify points with the highest Rankine mechanical net power  $P_{w_{mNet}}$  defined by equation 3.

Figure 4 presents an example of Rankine mechanical net power versus pump speed and expander speed obtained for an operating condition of  $20^{\circ}C$  ambient temperature, 2.5 m/s air velocity at the radiator,  $90^{\circ}C$  coolant temperature, 1500 l/h HT coolant flow rate and 1200 l/h LT coolant flow rate.

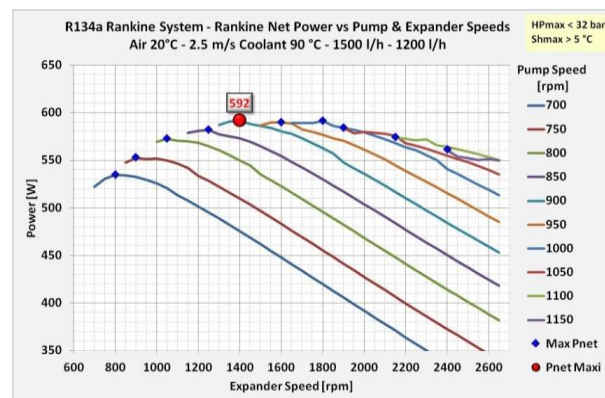


**Figure 4 :** Rankine net power for condition :

$$T_{aExt} = 20^{\circ}C \quad V_{aExt} = 2.5 \text{ m/s} \quad T_{cEvpi} = 90^{\circ}C \quad Q_{V_{Evpi}} = 1500 \text{ l/h} \quad Q_{V_{Cnd}} = 1200 \text{ l/h}$$

The blue dot points represent for a given pump speed, the expander speed with the maximum Rankine net power. The red dot point represents the optimal pump speed and optimal expander speed with the highest possible Rankine net power.

The next two figures present for the optimal Rankine net power obtained for different operating conditions. Figure 5a presents the effect of high temperature coolant loop temperature varying from 80°C to 115°C and for two ambient air temperatures of 20°C and 0°C. Figure 5b presents the effect of ambient air temperature variation from -20°C to 35°C for two high temperature coolant temperatures of 90°C and 110°C.



**Figure 5 :** Effect of operating conditions on optimal Rankine system performance  
 a: HT coolant temperature effect b: Ambient air temperature effect

As expected, the Rankine net power increases when the coolant temperature increases and when the ambient air temperature decreases. The Rankine net power vary from 339W at 35°C Ambient temperature and 90°C coolant temperature to 2155 W for -20°C ambient temperature and 110°C coolant temperature.

We can observe also that for a coolant temperature higher than 105°C, the slope of variation of the net power decreases. This is due to the limitations in high pressure  $HP_{work,max}$ . For example, at ambient air of 20°C, and coolant temperature of 110°C, the maximum Rankine net power without limitation in high pressure is 1005 W with a high pressure of 37 bars to be compared to 942 W with high pressure limited to 32 bars or 815 W with high pressure limited to 28 bars.

## 5 RANKINE SYSTEM CONTROL ALGORITHM

As stated in §4.1, the objective of the Rankine control system is to control the refrigerant pump speed and the expander speed in order to maximize the recovered net power  $P_{w,mNet}$  and protect the system during operating.

Quoilin, S., (2011) propose three control strategy of a small-scale ORC based on the regulation of evaporating temperature and superheating in order to control the expander and the pump speeds. A relationship of optimal evaporating temperature is defined by a linear regression of optimal results obtained from a set of 31 steady state workings points where condensing temperature, working fluid mass flow rate and heat source temperature are varying in certain range. The superheating is imposed to a constant value.

The control strategies developed in this paper are based on an estimation of the optimal evaporating high pressure and the optimal condensing low pressure, and they are also based on the high pressure limit and the minimal superheat limit. To estimate the optimal working points, we write down the equation of the recovered power in the evaporator, the rejected power in condenser, the shaft power produced by the expander and the power consumed by the pump. These equations are then simplified by using a set of assumptions. An analytical treatment allows us to define optimal roots that maximize the Rankine net power.

### 5.1 Expander speed control.

To control the expander speed, we estimate an evaporating high pressure set point  $P_{rEvpo\_sp}$  corresponding to the optimal evaporator power recovered from high temperature coolant loop  $P_{W_{rEvpo\_Opt}}$ . To do that, we set a number of assumptions in order to simplify the equation of  $P_{W_{mNet}}$ . After derivation  $\partial P_{W_{mNet}} / \partial P_{W_{rEvpo}} = 0$  and assuming some parameters as constants, we obtain a solution  $P_{W_{rEvpo}}$  that maximize  $P_{W_{mNet}}$  of the form: (f is a defined function of  $T_{cEvpi}$ ,  $T_{aExt}$ ,  $Q_{VcEvpo}$ ,  $Q_{VcCnd}$ ,  $V_{aExt}$  and the system components characteristics)

$$P_{W_{rEvpo\_Opt}} = f(T_{cEvpi}, T_{aExt}, Q_{VcEvpo}, Q_{VcCnd}, V_{aExt}) \quad (4)$$

From  $P_{W_{rEvpo\_Opt}}$  of equation 4 we define the evaporating high pressure set point  $P_{rEvpo\_sp}$  that will be used to control the expander speed.

### 5.2 Refrigerant pump speed control

To control the pump speed, we estimate a condensing low pressure set point  $P_{rCndi\_sp}$  or a pressure ratio set point  $P_{rat\_sp}$  corresponding to the maximum expander net power  $P_{W_{mNet}}$ . To do that, we used the equation of  $P_{W_{mNet}}$  and the high pressure set point  $P_{rEvpo\_sp}$  defined in §5.1. After different mathematical manipulations and some assumptions to simplify the equations, we set the derivative  $\partial P_{W_{mNet}} / \partial P_{ratio} = 0$  and we obtain a solution  $P_{ratio\_sp}$  that maximize  $P_{W_{mNet}}$  of the form: (g is a defined function of  $P_{rEvpo\_sp}$ ,  $T_{aExt}$  and the system components characteristics)

$$P_{ratio\_sp} = g(P_{rEvpo\_sp}, T_{aExt}) \quad (5)$$

From  $P_{ratio\_sp}$  of equation 5 and  $P_{rEvpo\_sp}$  we define the condensing low pressure set point  $P_{rCndi\_sp}$  that will be used to control the pump speed.

### 5.3 Control system architecture

Figure 6 presents the diagram of the Rankine control system. For this control strategy we use the following sensor data:

- From vehicle control unit:
  - $T_{aExt}$  : Air temperature at low temperature radiator inlet
  - $V_{aExt}$  : Air velocity at low temperature radiator inlet
  - $Q_{VcEvpo}$  : High temperature coolant volume flow rate at evaporator inlet
- From Rankine system :
  - $T_{cEvpi}$  : High temperature coolant temperature at evaporator inlet
  - $P_{rExp_i}$  : Refrigerant pressure at evaporator outlet or at expander inlet
  - $T_{rExp_i}$  : Refrigerant temperature at evaporator outlet or at expander inlet
  - $P_{rExp_o}$  : Refrigerant pressure at expander outlet or at pump inlet

An evaporating high pressure set point  $P_{rEvpo\_sp}$  and a condensing low pressure set point  $P_{rCndi\_sp}$  are estimated by the control system. The high pressure is then regulated by controlling the expander speed and using the estimated high pressure set point. The low pressure set point and the condition on the minimum superheat are used to control the pump speed.

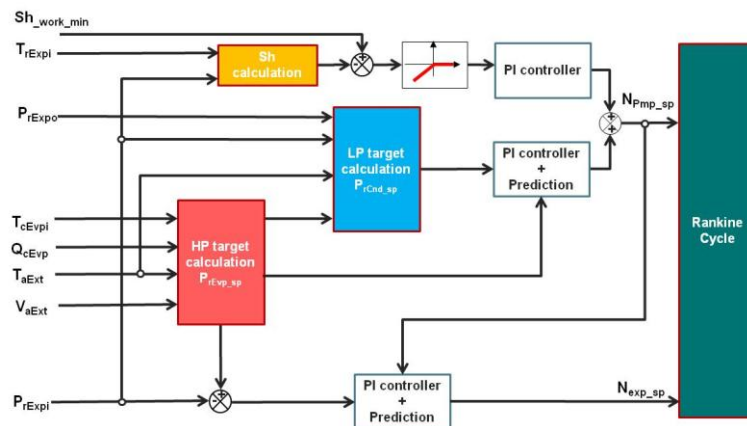


Figure 6 : Control system diagram

#### 5.4 Rankine control system validation.

Different algorithms to estimate the optimal evaporating high pressure and condensing low pressure were tested. In order to evaluate the performance of these algorithms, we tested the Rankine control system with the Rankine system alone without the vehicle model. Steady state simulations are performed on the matrix of operating conditions defined in §4.2.

Because of the assumptions and approximations used to estimate the optimal Rankine system working points, the Rankine net power obtained with the different control algorithms is, in general, lower than the reference net power. The differences are between 0 W to 40 W.

Figure 7 illustrates the performance of the selected control algorithm. The first graph 7a shows the comparison on the effect of evaporator coolant temperature from 80°C to 110°C. Ambient temperature is 20°C. The control allows us to obtain a very good level of Rankine net power with a maximum difference of 17 W corresponding to 3% compared to the optimal power. The second graph 7b shows the comparison on the effect of radiator air velocity from 0.75 m/s to 5 m/s. The maximum difference on Rankine net power is 20 W corresponding to 4% of the optimal power.

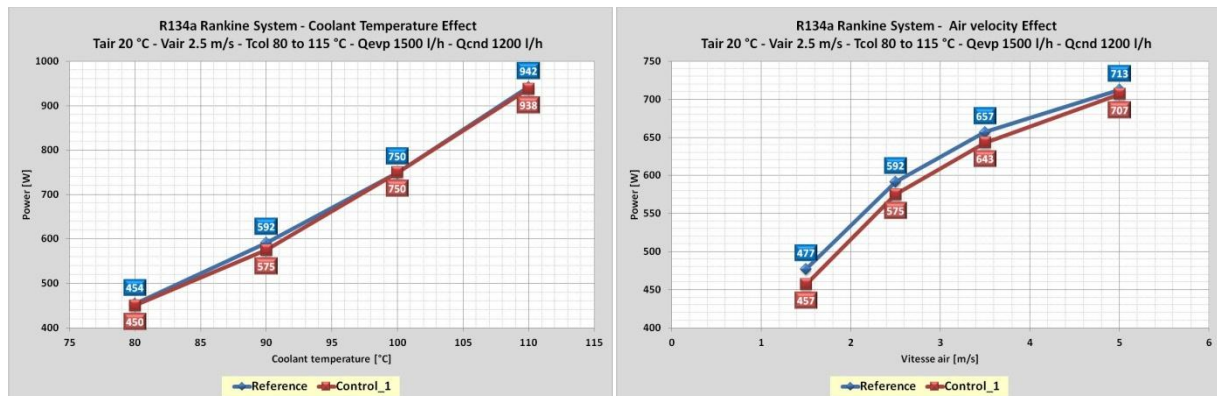


Figure 7 : Comparison of control algorithm performance on steady state conditions

## 6 VEHICLE INTEGRATION

### 6.1 Vehicle Energy and Thermal Management Simulation Platform

A simulation platform developed in the multi-physics systems simulation tool allows vehicle energy management and vehicle thermal management simulations of a vehicle equipped with a 2.0 liter turbocharged gasoline engine.

The R134a Rankine cycle model presented in Figure 2 and the control system were integrated into the Vehicle platform in order to simulate Rankine cycle with operating conditions close to real life

vehicle conditions. The interactions between vehicle and Rankine system are taken into account. However, in this study, the use of recovered power by the Rankine system electrically or mechanically by the vehicle power train is not considered. We only evaluate the recovered mechanical net power. The use of this power will be up to the carmaker strategy and will depend on the vehicle and the power train architecture and engine control strategy.

## 6.2 Application to constant velocities driving cycles

Figure 8 presents the Rankine net power obtained for constant vehicle velocities from 30 km/h to 180 km/h and for ambient temperature from  $-10^{\circ}\text{C}$  to  $25^{\circ}\text{C}$ . The thermostat temperature setting is  $90^{\circ}\text{C}$ .

The following remarks can be stated:

- The Rankine net power increases when the vehicle speed increases. This is due to an increase of the available waste heat that can be recovered by the evaporator on one side, and an improvement of condensation performance due to the radiator air velocity increases with vehicle velocity on the other side.
- The Rankine net power is higher for low ambient temperature than for high ambient temperature. This is due to the improvement of condensation performance.
- The Rankine net power is limited by the recovered heat which is limited by the condensation side of the system, the pump and expander size.

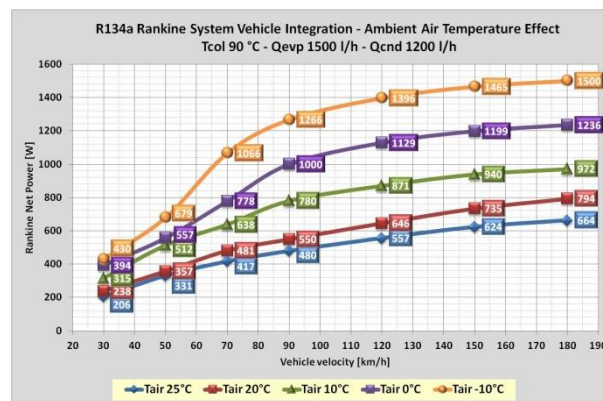


Figure 8 : Rankine net power versus vehicle speed and ambient air temperature

## 6.3 Application to transient driving cycle

To illustrate the performance of the Rankine control system, results are presented for transient WLTC driving cycles. WLTC is the driving cycle of the upcoming Worldwide harmonized Light vehicle Test Cycle. WLTC is more representative of real life driving in urban and sub urban conditions than driving cycles like NEDC. The duration of the WLTC cycle is 1800s and the average vehicle velocity is 46 km/h with a maximum vehicle velocity of 130 km/h. The simulations are performed for a period of 3600 s corresponding to two times the WLTC cycle duration in order to compare a WLTC with cold start engine and a WLTC cycle with warm engine.

Figure 9 presents the evolution of different Rankine cycle variables during the two WLTC driving cycles at  $10^{\circ}\text{C}$  ambient temperature. We can distinguish different phases:

- Phase I: At the start of the driving cycle, we assume that the vehicle temperature is constant and equal to the ambient temperature of  $10^{\circ}\text{C}$ . During the first 780 s period, the engine and the coolant are not hot enough and the Rankine system is switched off. The expander speed is zero and the pump speed is zero (In fact, for numerical reasons, the pump speed is set to a small value in order to ensure a minimal refrigerant circulation)
- Phase II: The coolant temperature is now higher than a coolant temperature high limit setting of  $85^{\circ}\text{C}$ , the Rankine system is activated and the pump and the expander are controlled in order to



regulate high pressure set point and low pressure set point with the constraint on minimum superheat  $Sh_{work\_min}$ .

- Phase III (highlighted zones): The vehicle speed is too low or the vehicle is stopping. There is no more sufficient energy to be recovered. The air velocity at the radiator vanishes unless we switch on the Fan. The coolant outlet temperature is decreasing and reaches a low temperature limit setting of 80°C. So, the Rankine system is switched off and the pump and the expander are stopped.

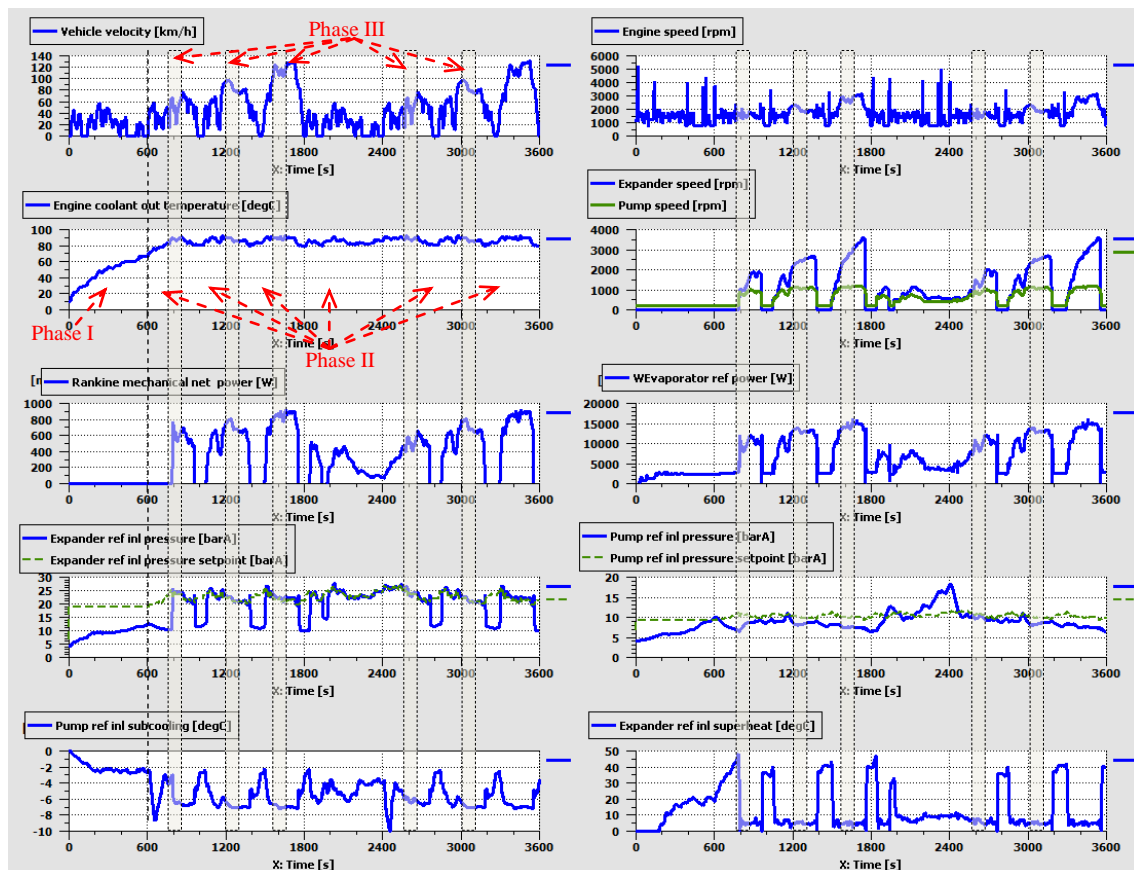
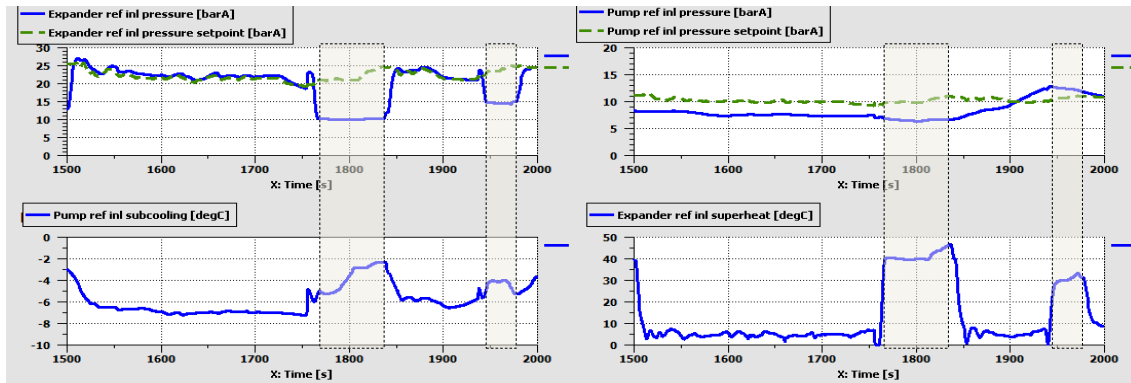


Figure 9 : Rankine system operation during WLTC driving cycle

Figure 10 presents a zoom showing the performance of the regulation of the evaporating high pressure and the condensing low pressure. The first graph shows the regulation of evaporation high pressure. The simulated high pressure follows correctly the estimated high pressure evolution defined by the control system with a delay of about 5s. The high pressure drops down when the Rankine system is switched off and the expander is stopped. The second graph presents the control of condensation low pressure. The condensing low pressure is 3 to 4 bars lower than the optimal low pressure defined by the control. In fact, to increase the level of low pressure we need to increase the pump speed. However, the superheat is very low as shown in the fourth graph. If the pump speed increases, the superheat will decrease below the  $Sh_{work\_min}$  limitation. So, during these operating conditions the pump speed is controlled here by the superheat limit instead of by the condensation low pressure.



**Figure 10 :** Evaporating high pressure and condensing low pressure control

## 7 CONCLUSION

In this paper, we presented a methodology to develop and validate a control system of a low temperature waste heat recovery Organic Rankine Cycle system based on a co-simulation between a control tool and a systems simulation tool.

In the first part, a model of R134a Rankine cycle developed in a multi-physics systems simulation tool is presented. The model is based on a R134a Rankine prototype developed and tested at Valeo on a test bench. Experimental results obtained on the prototype are used to set up, calibrate and validate the models of the components and the Rankine system models.

The Rankine system model is then integrated into a global vehicle energy and thermal management model allowing simulation of Rankine system in various vehicle operating conditions corresponding to constant vehicle velocities.

A control algorithm is derived from an analytical analysis of the Rankine system equations. Different estimation of optimal evaporating high pressure and condensing low pressure are extracted and used to control the expander speed and the pump speed. The control algorithm programmed in a control tool is coupled to the physical model of a vehicle with Rankine system. The selected control algorithm was validated in steady state conditions and showed a good performance. The estimated Rankine net power obtained with the control system is no more than 20 W lower than the maximum possible net power.

Finally, the Rankine control system is applied to a transient WLTC driving cycle at different ambient conditions. It shows the ability of the control system to regulate the Rankine system with highly transient external and internal operating conditions in order to maximize the recovered mechanical net power and ensure a good conditions for a safe Rankine system functioning.

The developed control strategy and the methodology presented here can be adapted to different Rankine cycle architectures and different working fluids. It allows us also to study and evaluate different vehicle integration architectures and different options to use the mechanical power recovered by the expander directly to assist the engine and bring part of the power needed to accessories functioning or indirectly by producing electricity with an electrical generator.

## NOMENCLATURE

$Eff_{mExp}$	Expander mechanical efficiency	[-]
$HP_{work\_max}$	High pressure maximal working limit	[barA]
$H_{rExpi}$	Refrigerant enthalpy at expander inlet	[J/kg]
$H_{rExpO}$	Refrigerant enthalpy at expander outlet	[J/kg]
$P_{ratio\_sp}$	Ratio of high and low pressure set point	[-]
$P_{rCndi\_sp}$	Refrigerant pressure set point at condenser inlet	[barA]
$P_{rEvpo\_sp}$	Refrigerant pressure set point at evaporator outlet	[barA]

$P_{rExp_i}$	Refrigerant pressure at expander inlet	[barA]
$P_{rExp_o}$	Refrigerant pressure at expander outlet	[barA]
$P_{W_{mExp}}$	Expander mechanical power	[W]
$P_{W_{mNet}}$	Rankine mechanical net power	[W]
$P_{W_{rEvap}}$	Evaporator refrigerant power	[W]
$P_{W_{rEvap\_Opt}}$	Optimal evaporator refrigerant power	[W]
$Q_{m_{rExp}}$	Expander refrigerant mass flow rate	[kg/s]
$Q_{V_{cCnd}}$	Coolant volume flow rate at condenser inlet	[m <sup>3</sup> /s]
$Q_{V_{cEvap}}$	Coolant volume flow rate at evaporator inlet	[m <sup>3</sup> /s]
$S_{b\_work\_min}$	Subcooling minimal working limit	[K]
$S_{h\_work\_min}$	Superheat minimal working limit	[K]
$T_{aExt}$	Ambient air temperature	[°C]
$T_{cCnd_i}$	Coolant temperature at condenser inlet	[°C]
$T_{cCnd_o}$	Coolant temperature at condenser outlet	[°C]
$T_{cEvap_i}$	Coolant temperature at evaporator inlet	[°C]
$T_{cEvap_o}$	Coolant temperature at evaporator outlet	[°C]
$T_{rExp_i}$	Refrigerant temperature at expander inlet	[°C]
$T_{rExp_o}$	Refrigerant temperature at expander outlet	[°C]
$T_{rPmp_i}$	Refrigerant temperature at refrigerant pump inlet	[°C]
$T_{w\_out\_min}$	Coolant temperature return minimal working limit	[°C]
$V_{aExt}$	Air velocity at low temperature radiator inlet	[m/s]

## REFERENCES

- El Habchi, A., Ternel, C., Leduc, P., Hetet, J.F., 2010, Potential of waste heat recovery for automotive engines using detailed simulation, *ASME-ATI Conference on Thermal and Environment Issues in Energy Systems, Sorrento, Italy, May 16-19*.
- Abbe Horst, T., Tegethoff, W., Eilts, P., Koehler, J., 2014, Prediction of dynamic Rankine Cycle Waste heat recovery performance and fuel saving potential in passenger car applications considering interactions with vehicles energy management, *Energy Conversion and Management, vol. 78, p. 438-451*.
- Domingues, A., Santos, H., Costa, M., 2013, Analysis of vehicle exhaust waste heat recovery potential using a Rankine Cycle, *Energy vol. 49 p. 71-85*.
- Haller, R., Nicolas, B., Hammi, S., Taklanti, A., Labaste-Mauhe, L., Glavatskaya, Y., Yahia, M., 2014, Comparison of high and low temperature working fluids for automotive Rankine waste heat recovery systems, *SIA Powertrain, Rouen, France, May 21-22; 2014*.
- Taklanti, A., Liu, J.M., Yahia, M., 2013, Toward verification and optimization of electrical vehicle thermal management control strategies based on virtual vehicle model, *SAE Thermal Management Systems Symposium, Troy, Michigan October 22-24; 2013*.
- Quoilin, S., Aumann, R., Grill, A., Schuster, A., Lemort, V., Spliethoff, H., 2011, Dynamic modeling and optimal control strategy of waste heat recovery Organic Rankine Cycles, *Applied Energy vol. 88 p 2183-2190*.